



Finite Element Mesh Generation for Nano-scale Modeling of Tilted Columnar Thin Films for Numerical Simulation

Noé Watiez¹(✉), Aurélien Besnard¹, Pavel Moskovkin², Ruding Lou³, José Outeiro¹,
Hélène Birembaux¹, and Stéphane Lucas²

¹ Arts et Métiers Institute of Technology, LaBoMaP, 71250 Cluny, France
noe.watiez@ensam.eu

² University of Namur, 5000 Namur, Belgium

³ Arts et Métiers Institute of Technology, LISPEN, 71100 Chalon-sur-Saône, France

Abstract. Glancing Angle Deposition (GLAD) is a technique used in Physical Vapor Deposition (PVD) to prepare thin films with specific properties. During the deposition process, a tilt is introduced between the sputtered atoms flux and the normal of the substrate surface. By shadowing effect, this induces tilted nano-columns that affect the properties of the coating. To predict these properties, several existing tools simulate the different steps of the PVD deposition. First, a simulation of the sputtering of atoms from a metallic target is made, followed by the computation of the atoms transportation from the target to the substrate. Finally, the growth of the film is computed. All these simulations use point based representation to represent the deposited atoms. However, such representation is not suited for classical finite elements analysis (FEA).

In this paper, a methodology for generating FEA meshes from the points produced by film growth simulation is presented. Two major scientific challenges are overcome. Firstly, how to segment the “film” point cloud into a collection of individual “columns” and secondly, how to generate the meshes of the columns that are approximately represented by points. The point cloud segmentation is computed through neighbourhood notion. The mesh is obtained as an implicit surface by the marching cubes algorithm and smoothed by a Humphrey’s class Laplacian algorithm. Numerical simulations based on the generated FEA meshes will be conducted using Abaqus FEA software.

Keywords: PVD · GLAD · Columns · FEM · Simulation · Point cloud · Meshes

1 Introduction

Physical Vapor Deposition (PVD) is a process used to coat parts with thin layers ranging from a few hundreds of nanometers to a few micrometers in thickness. It has a large scale of application due to a high degree of freedom in the composition of the layer as well as an easy application in the industry [1]. It is used in several domains, ranging

from mechanical application (such as coated milling drills) [2], optics [3], electronics [4] and in several other fields.

The deposition is carried out at an atomic scale in a vacuum chamber, hence *in situ* data is sparse [5]. Most of the information comes from post-deposition characterization of the coating [1]. In this case, simulation is a key to evaluate the macroscopic properties from several micro-scale interaction through laws of physics.

Many simulation software are based on the Monte-Carlo algorithm, and, in particular Kinetic Monte-Carlo (KMC). Different successive codes are mandatory to conduct such study. For example, SRIM [6] or TRYDYN [7] can be used to characterize the sputtering from a target, SIMTRA [8] computes the transportation of matter in the chamber, NASCAM [9, 10] or SIMUL3D [11] simulate the growth of the columnar film. This list is not exhaustive, however it presents the three type of software used in PVD simulation (sputtering, transport, growth). However, no software currently support the mechanical simulation of thin films based on a simulated structure. The aim of this study is to address this lack and produce such simulation.

This paper presents a pilot study of FE meshes generation from point based film growth simulation result which will be used in Finite Element Method (FEM) simulation of the mechanical properties.

2 Technological background

2.1 Presentation of the GLAD Process

As its name implies, PVD process uses the physical phenomenon in order to turn the solid material into a vapor, which is then deposited onto the part. The phenomenon used in this study is called “Magnetron Sputtering”.

Figure 1 presents the PVD process: in a deposition chamber, a plasma is condensed on the surface of a metal object, called target, which leads to the erosion of the surface and the sputtering of the eroded matter. Then, the sputtered matter is transported through the chamber toward a substrate, resulting in the growth of the film.

This study focuses particularly on the GLancing Angle Deposition process (GLAD) in which an angle is formed between the flux of sputtered matter and the substrate in order to constrain the growth. The major effect is the apparition of an inclined porous columnar structure due to the shadowing effect as presented by Hawkeye *et al.* [12]. It is then possible to nanostructure the film by controlling the deposition angle and thus vary its properties. This effect has already been documented for a variety of applications, such as anti-reflect optical films [13], magnetic films [14] or mechanical applications [15].

2.2 Simulation Steps

The current steps of the simulation is the successive simulation of the sputtering, the transport and the growth of the film [16]. In this study, the sputtering step is conducted with SRIM [5] and SIMTRA [8]. The former estimates the atom flux resulting from the ion and the target in both angle and energy in a localized manner (a few nm² surface of the target). Whereas the latter uses those angular and energetic distribution as well as a racetrack in order to create the emission overall the target.

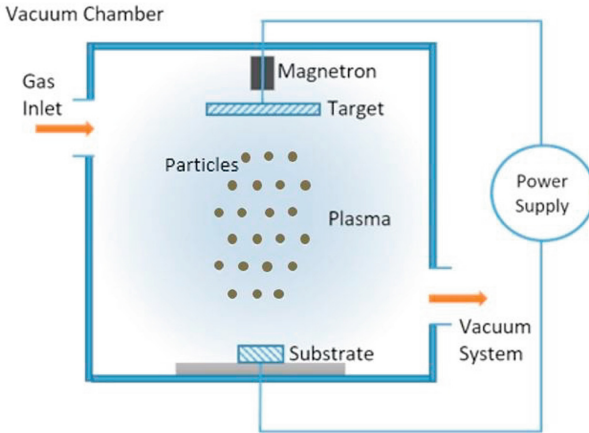


Fig. 1. Outline of the PVD process [2]

SIMTRA then proceeds to the computation of the transportation in the chamber, considering the collisions with the atoms present, in this case argon at a pressure of 2.2×10^{-3} mbar, and returns a file containing the final position, angle and energy of any atom landing on the target.

Finally, NASCAM [8, 9] simulates the growth from the transportation result given by SIMTRA. Several transportations can be used together to emulate multi-target deposition as well as a reactive atmosphere. It results into a point clouds on a cubic or hexagonal grid with information about the composition and the morphology. The three software are based on the KMC algorithm.

This paper presents a post-processing workflow made to prepare the results from the previously stated simulation for mechanical calculation by finite element model.

3 Post-processing

The construction of a mesh from the simulated PVD growth consists of several steps. The overall workflow of the process is presented in Fig. 2. The state of the input and output data is also provided between each two successive steps. The following parts elaborates on the column separation algorithm as well as the steps followed in order to produce a smooth mesh from the point cloud computed for each column morphology in the initial simulation step. The mesh assembly consists of simply adding all sub-meshes for each column to a global coating mesh.

3.1 Columnar Separation

As previously stated, the GLAD technique induces a columnar morphology, which in turn causes variations of the film properties. Hence, in order to compute the film properties, it is necessary to study the columns. This is the aim of the first part of the post-processing algorithm. NASCAM exports a point cloud where each point represents an atom and

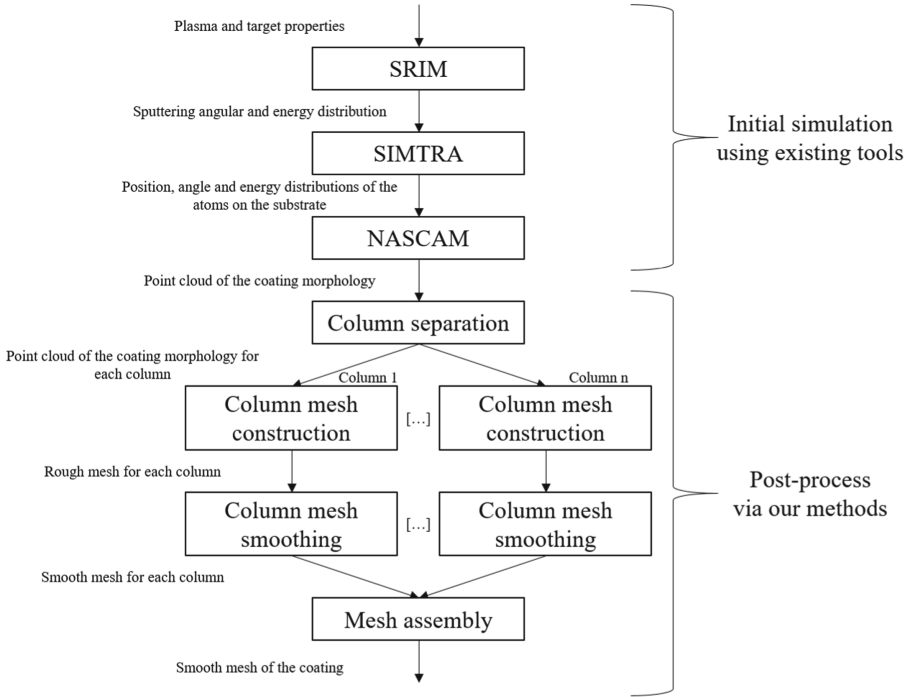


Fig. 2. Workflow of the simulation from the PVD process to the construction of the mesh

possesses the name of the chemical specie in addition to the xyz coordinates. Unfortunately, no information about the point clustering according to the columns is provided. Therefore, a method has to be designed to segment this global point cloud into a set of columns.

The designed method is based on the growth of a column and the chronological flux of atoms. Figure 3 illustrates three principal cases when an atom arrives on the substrate. If the atom arrives on the substrate without any neighbor, a new column is created (Fig. 3a). Else, the atom is added to one of the column from its neighbors. If there is only one neighbor atom, the newly arriving atom will belong to the same column of this unique neighbor (Fig. 3b). If the newly arriving atoms is in contact to several neighbors belonging to different columns, the one of highest weight is assigned to the newly arriving atom (Fig. 3c).

Figure 4 is a logic graph presenting the major steps of the column separation algorithm.

All neighbors are considered by relative attraction, which means with a decay along the distance to the point. For calculation purpose and according to the work on a cubic grid, only the points contained in the cube of three units edges centered on the newly added point are considered as neighbors as presented in Fig. 5.

In this figure the neighboring positions to any point on the grid, here the orange point with a halo are filled with virtual points. A color is given to each in accordance with the distance from this point to the central point. Positions on the faces (pink) are at the

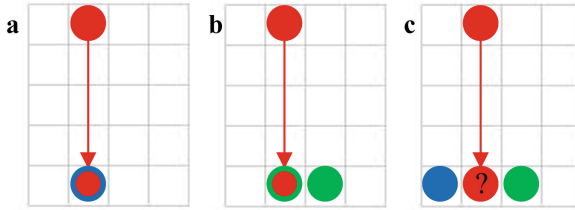


Fig. 3. Schematic representation of the attribution of an atom depending on the neighboring structure. (a) No neighbors, (b) A single neighbor, (c) several neighbors

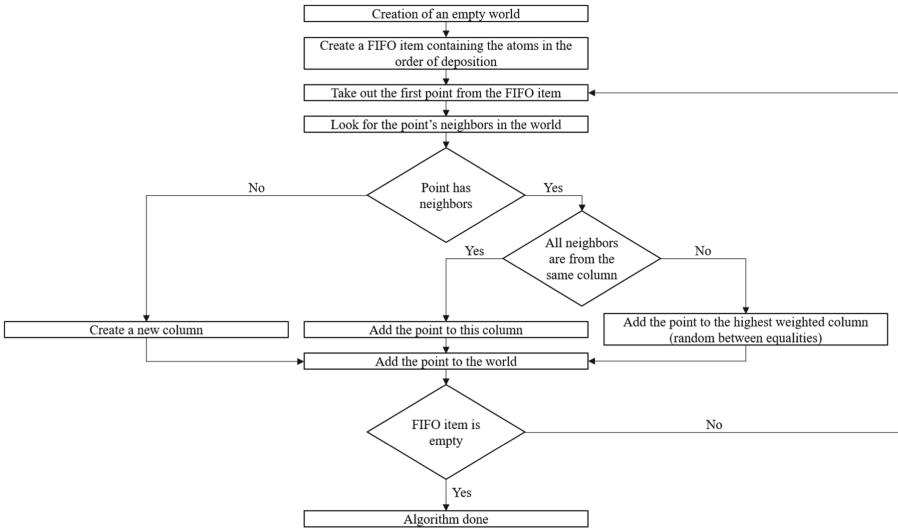


Fig. 4. Logic graph of the algorithm

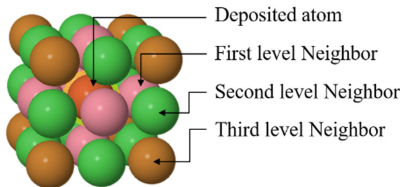


Fig. 5. Layout of the neighborhood of an atom in the algorithm

distance of 1 unit, on the edges (green) at $\sqrt{2}$ units and on the vertices (brown) at $\sqrt{3}$ units. In a first approximation, the parameters used by Besnard [17] on Simul3D will be kept for further simulation. It estimates the weight of any point to be linear with its inverted distance to the middle of the cube.

In order to develop the algorithm, it is necessary to know the structure around every point at the time of deposition. A new option implemented in NASCAM provides the

deposition order and the successive position of each point. By browsing through this file, it is possible to have the structure at any time of the deposition.

NASCAM works in a prismatic world. To reduce computational costs, this world is periodic: its boundary planes along both the x and the y axis are considered adjacent. This has to be taken into account in the separation of columns as one can overlap over different boundaries of the world, mostly in highly tilted deposition (Fig. 6).

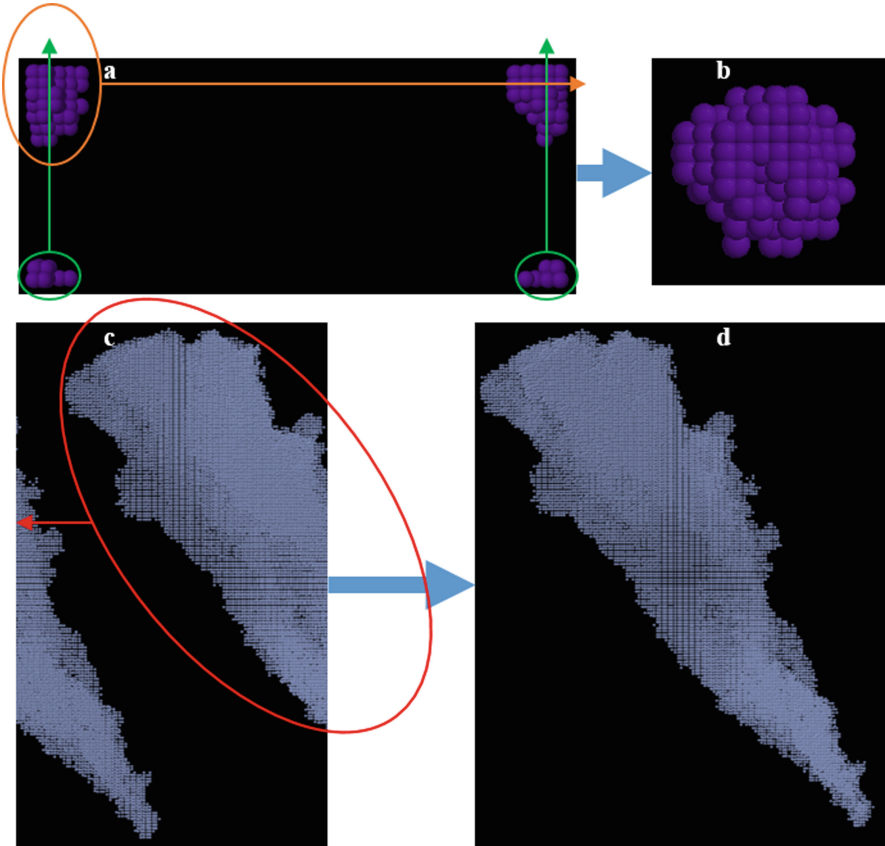


Fig. 6. Top view of a small column on a periodic world along with the steps needed for the deperiodicization (a) and of the same column in a non periodic world. Cross section of a large column in a periodic (c) and non-periodic (d) world

Figure 6a presents the effect of the periodicity on the top view of a single small column and Fig. 6b show the shape of the same column in a non-periodic world. Figure 6c and d present the same situation for a large column in cross section view.

The results of the column separation algorithm are presented on Fig. 7.

Figure 7a presents the raw structure exported by NASCAM, while Fig. 7b presents the segmented structure where columns are identified and displayed in different colors. It can be observed that, in accordance with the literature [13], the lower part of the

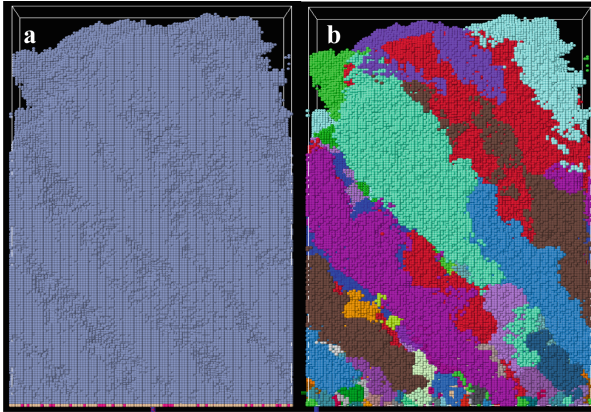


Fig. 7. Comparison of raw data from Nascam (a) and columnar separation algorithm (b)

structure mostly consists of densely packed small columns and the higher part are made of sparsely located large columns due to the shadowing effect [12].

3.2 Mesh Construction

The point cloud could not be used as it is for classic FEM mechanical calculation. Although point based mechanical simulations exist in the literature [18], it has been preferred for this study to work with FEM simulation software, which requires the construction of a mesh.

Concerning this point, several choices were made:

- Ignoring the internal porosities of the columns, which would be considered as computation artefacts from the probabilistic approach.
- Creating a mesh on an implicit surface set so that the surfaces created around adjacent points from different columns are in contact.
- Smoothing the mesh to improve the computability and to reduce the serrated patterns induced by the voxelization used in NASCAM.

The suppression of the internal porosities is made through the Ball Pivoting algorithm [19] in which a ball of given radius rolls on the edges, creating a triangle surface when it is in contact with three points. The created surface is then voxelized [20]. From these two steps, a new point cloud is obtained which presents no porosity nor holes smaller than the ball radius. Figure 8b presents a slice of the point cloud corresponding to the dark blue column on the data exported from NASCAM (Fig. 8a) with two added cavities, one on the surface and one in the bulk. Figure 8c corresponds to the slice of the point cloud obtained after applying a voxelization algorithm to the surface created by Ball Pivoting and filling the voxelized data. These two steps reduce the impact of surface cavities depending on the size of the ball chosen for the algorithm and guaranty the density of the columns.

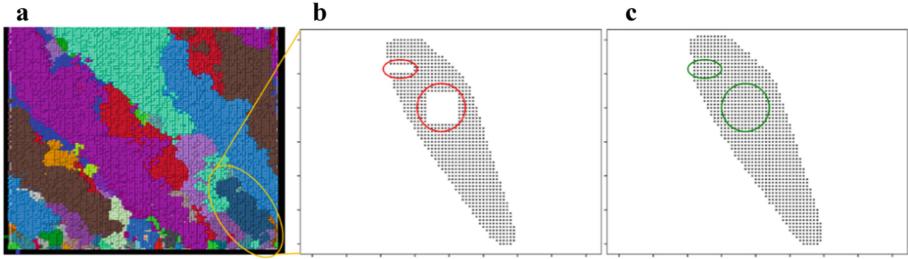


Fig. 8. Raw (a) and densified (b) point clouds representing a column

The implicit surface mesh is then constructed through the Marching Cubes algorithm [21, 22] applied to the voxelized point cloud. A cube is moved through the point cloud adding edges and surfaces by comparing the position of the points in the cube to a library of all possibilities. Thanks to this structure, this algorithm is fast and reliable on dense point clouds but very prone to errors in sparse ones. It is an efficient solution given the previous assumption to consider columns as dense entities.

Due to the fact that Marching Cube algorithm uses predetermined structure on a grid, the range of possible angles between surfaces are limited, sometime resulting in sharp angles, ill-suited for mechanical calculation. The Fig. 9a presents a slice of the surface constructed by Marching Cubes from the column highlighted in Fig. 8a. As expected, the grid parameters are obvious and the structure is very serrated along oblique angles.

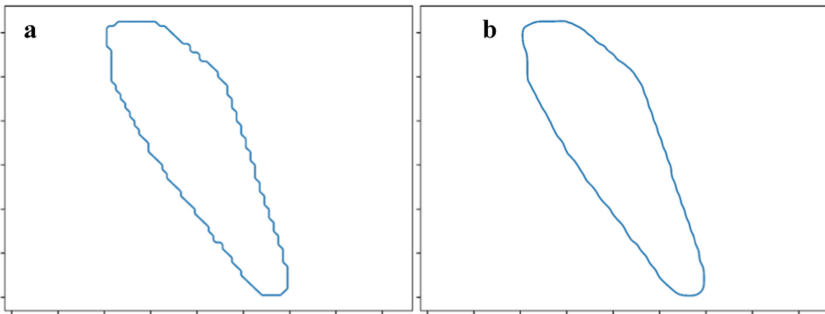


Fig. 9. Slice of the mesh created by the Marching Cubes algorithm from the dense point cloud presented in 7c corresponding to the column highlighted in 7a, before smoothing (a) and after smoothing (b)

Consequently, a smoothing is applied to reduce the impact of the grid. The Humphrey's Class Laplacian Smoothing [23] is used in order to produce a smooth mesh while at the same time limiting the volume shrinkage of the bulk. Nevertheless, a reduction of the global volume is still to be expected in the sharp boundaries. Volume measurement points to a loss of approximately 3% in volume. The smoothing has very little impact on the bulk.

As can be seen on Fig. 9b, the structure is mostly conserved with only a few rounder angles or straighter oblique edges replacing the serrated ones.

The 3D rendering of the column's mesh on the software Blender is presented in Fig. 10.

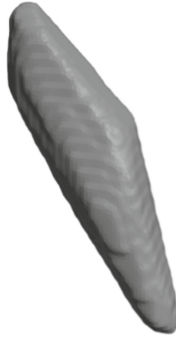


Fig. 10. 3D mesh of a simulated PVD column

At this point, it is possible to import the resulting mesh into a FEM calculator to compute the mechanical properties but the real interest comes from the possibility to create an assembly from all the columns of a given deposition simulation and run the calculation for the whole coating.

Figure 11 presents a side by side an SEM (Scanning Electron Microscopy) image of a coating and the assembly of the columns from the simulated world shown on Fig. 7 created by the application of the proposed 3D reconstruction method. The reconstructed structure is similar to the SEM images of a similar coating, both on the measured column tilt and on the shape of the columns, which involve multiple thin columns at the base and a few large columns at the top.

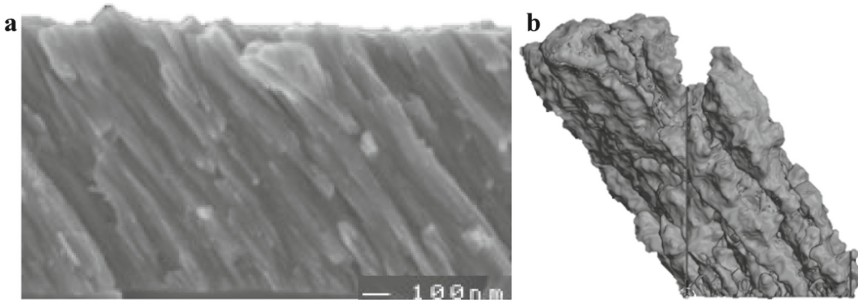


Fig. 11. (a) SEM image of a GLAD coating (b) 3D mesh of a simulated PVD world

4 Conclusion and Perspectives

This study presents a method devised from the numerical simulation of thin film growth to the construction of the FE mesh. This method has been successfully conducted in

a two step-approach. The first step is a segmentation of the film in a set of columns while the second step consist in the creation of surface meshes for each column. The 3D representation of the current meshes shows consistency with experimental data obtained by SEM microscopy on both the tilt and the shape of the columns.

The process will be perfected in a batch of experimental and numerical investigations of the morphological (SEM) and mechanical (nano-indentation tests) properties of thin films.

The parameters expected to be reviewed this way are:

- The weight of the face, edge and vertex atoms in the definition of the attribution of a new deposited atom to the existing columns. The parameter presently used is a reduction proportional to the inverted distance as suggested by Besnard's previous work [17].
- The size of the mesh unit, which is currently based on the grid from NASCAM.
- The number of successive smoothing which may be increased or decreased depending on the computational capabilities of the machine.

Another potential upgrade factor for this study is the risk of collision between columns during the assembly part due to the shape modification from the smoothing.

Although the smoothing mostly induces a reduction of the shape in the boundaries, it may result in local expansions. In the case of this happening in the boundary between adjacent columns, it could lead to collisions and failure of the simulations, an additional part could be included at the assembly step to resolve the issue in those situations.

References

1. Martin, P.M.: Handbook of Deposition Technologies for Films and Coatings, third edition. Cambridge, Elsevier, p. 936 (2010). ISBN 978-0-8155-2031-3
2. Baptista, A.: On the physical vapour deposition (PVD): evolution of magnetron sputtering processes for industrial applications. *Procedia Manuf.* **17**, 746–757 (2018). <https://doi.org/10.1016/j.promfg.2018.10.125>
3. Stoessel, C.H.: Optical Thin Films and Coatings (Second Edition), Woodhead Publishing, p. 860 (2018). ISBN 978-0-08-102073-9
4. Ma, Y.: Materials and structure engineering by magnetron sputtering for advanced lithium batteries. *Energy Storage Mater.* **39**, 203–224 (2021). <https://doi.org/10.1016/j.ensm.2021.04.012>
5. Bobzin, K.: Enhanced PVD process control by online substrate temperature measurement. *Surf. Coat. Technol.* **354**, 383–389 (2018). <https://doi.org/10.1016/j.surfcoat.2018.07.096>
6. Ziegler, J.F.: “SRIM-2003”, Nuclear Instruments and Methods in Physics Research B, vol. 219–220, pp. 1027–1036 (2004). <https://doi.org/10.1016/j.nimb.2004.01.208>
7. Möller, W.: Tridyn-binary collision simulation of atomic collisions and dynamic composition changes in solids. *Comput. Phys. Commun.* **51**, 355–368 (1998). [https://doi.org/10.1016/0010-4655\(88\)90148-8](https://doi.org/10.1016/0010-4655(88)90148-8)
8. Aeken, K.V.: The metal flux from a rotating cylindrical magnetron: a Monte Carlo simulation. *J. Phy. D: Appl. Phys.* **41**, 205307 (2008). <https://doi.org/10.1088/0022-3727/41/20/205307>
9. Lucas, S., Moskovkin, P.: Simulation at high temperature of atomic deposition, islands coalescence, Ostwald and inverse Ostwald ripening with a general simple kinetic Monte Carlo code. *Thin Solids Films* **518**, 5355–5361 (2010). <https://doi.org/10.1016/j.tsf.2010.04.064>

10. Moskovkin, P., Lucas, S.: Computer simulations of the early stage growth of Ge clusters at elevated temperatures, on patterned Si substrate using the kinetic Monte Carlo method. *Thin Solids Films* **536**, 313–317 (2013). <https://doi.org/10.1016/j.tsf.2013.03.031>
11. Besnard, A., Martin, N., Carpentier, L.: Three-dimensional growth simulation: a study of substrate oriented films. *Mater. Sci. Eng.* **12**, 012011 (2010). <https://doi.org/10.1088/1757-899X/12/1/012011>
12. Hawkeye, M.M.: *Glancing Angle Deposition of Thin Films: Engineering the Nanoscale*, p. 320 Wiley, Hoboken (2013). ISBN 978–1–118–84756–5
13. Lacroix, B.: Nanostructure and physical properties control of indium tin oxide films prepared at room temperature through ion beam sputtering deposition at oblique angles. *J. Phys. Chem. C* **123**, 14036–14046 (2019). <https://doi.org/10.1021/acs.jpcc.9b02885>
14. Potočník, J.: The influence of thickness on magnetic properties of nanostructured nickel thin films obtained by GLAD technique. *Mater. Res. Bull.* **84**, 455–461 (2016). <https://doi.org/10.1016/j.materresbull.2016.08.044>
15. Lintymer, J.: Influence of zigzag microstructure on mechanical and electrical properties of chromium multilayered thin films. *Surf. Coat. Technol.* **180–181**, 26–32 (2004). <https://doi.org/10.1016/j.surfcoat.2003.10.027>
16. Siad, A. : *Etude numérique et expérimentale de la croissance de couches minces déposées par pulvérisation réactive* (2016). tel-01418118
17. Besnard, A.: Three-dimensional growth simulation: A study of substrate oriented films. In: *IOP Conference Series: Materials Science and Engineering*, vol. 12 (2010). <https://doi.org/10.1088/1757-899X/12/1/012011>
18. Kudela, L.: Direct structural analysis of domains defined by point clouds. *Comput. Methods Appl. Mech. Eng.* **358**, 112581 (2019). <https://doi.org/10.1016/j.cma.2019.112581>
19. Bernardini, F.: The ball-pivoting algorithm for surface reconstruction. *IEEE Trans. Vis. Comput. Graph.* **5**, 349–359 (1999). <https://doi.org/10.1109/2945.817351>
20. Lai, S., Cheng, F.: Voxelization of free-form solids represented by catmull-clark subdivision surfaces. In: Kim, M.-S., Shimada, K. (eds.) *GMP 2006*. LNCS, vol. 4077, pp. 595–601. Springer, Heidelberg (2006). https://doi.org/10.1007/11802914_45
21. Lorensen, W.: Marching cubes: a high resolution 3D surface construction algorithm. *Comput. Graph.* **21**, 163–169 (1987). <https://doi.org/10.1145/37402.37422>
22. Lewiner, T.: Efficient implementation of marching cubes' cases with topological guarantees. *J. Graph. Tools* **8**, 1–15 (2003). <https://doi.org/10.1080/10867651.2003.10487582>
23. Vollmer, J.: Improved laplacian smoothing of noisy surface meshes. *Comput. Graph. Forum* **18**, 131–138 (1999). <https://doi.org/10.1111/1467-8659.00334>